

# Fabrication and Characterization of the Plate-Shaped $\gamma$ -Fe<sub>2</sub>O<sub>3</sub> Nanocrystals

Yonghong Ni, Xuewu Ge,\* Zhicheng Zhang,\* and Qiang Ye

Department of Applied Chemistry, University of Science and Technology of China, Hefei, Anhui, 230026, People's Republic of China

Received May 3, 2001. Revised Manuscript Received October 19, 2001

Plate-shaped  $\gamma$ -Fe<sub>2</sub>O<sub>3</sub> nanocrystals have been successfully prepared in a water system by a simple reduction–oxidation method at room temperature and under ambient pressure. The reactions contain two steps: first, Fe(II) is reduced into Fe atoms by  $\gamma$ -ray irradiation in nitrogen atmosphere; then, Fe atoms are oxidized into  $\gamma$ -Fe<sub>2</sub>O<sub>3</sub> in air. XRD, TEM, EDXA, XPS, and Mössbauer spectrum were used to characterize the final product. The magnetic characterization showed that the  $\gamma$ -Fe<sub>2</sub>O<sub>3</sub> nanocrystals have a specific saturation magnetization of 83 emu/g and a coercivity of 320 Oe (25.5 kA/m). A possible formation mechanism of the plate-shaped  $\gamma$ -Fe<sub>2</sub>O<sub>3</sub> nanocrystals was suggested.

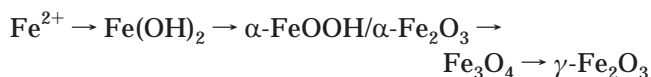
## 1. Introduction

The design and synthesis of various nanomaterials are the subjects of intense current research because of their special electronic, optical, magnetic, and physicochemical properties. Many techniques have been developed for the synthesis of nanoscale compounds with semiconductor nanocrystals in particular. However, relatively little work exists for magnetic materials of similar dimensions.<sup>1–3</sup> In recent years, the preparation of magnetic nanomaterials has gradually attracted much interest, since these materials have many potential applications in information storage, color imaging, bioprocessing, magnetic refrigeration, gas sensors, ferrofluids, and so on.<sup>4–10</sup> Among a variety of magnetic materials,  $\gamma$ -Fe<sub>2</sub>O<sub>3</sub> powders have been widely used for the longest period of time due to their excellent ferromagnetic properties.

It is well-known that water irradiated by  $\gamma$ -rays can generate many active particles such as hydrated electrons and hydrogen atoms, which can reduce metal ions to metal atoms owing to their strong reduction. Early in 1985, J. Belloni et al.<sup>11</sup> successfully obtained cobalt

and nickel nanoparticles from a colloid solution irradiated by  $\gamma$ -rays at the first time. Then, many noble metals, some nonnoble metals, or bimetallic alloys<sup>12–14</sup> were prepared by  $\gamma$ -ray irradiation technique at room temperature and under ambient pressure. In 1999, the above technique was employed to reduce  $\beta$ -FeOOH by S. Wang and H. Xin.<sup>15</sup> The yielded product proved to be nanocrystals of Fe<sub>3</sub>O<sub>4</sub>. In brief,  $\gamma$ -ray irradiation have been extensively used to prepare nanocrystalline metals, alloys, oxides, and sulfides in the past decade.<sup>12–16</sup>

The conventional route for the synthesis of  $\gamma$ -Fe<sub>2</sub>O<sub>3</sub> powders is the controlled oxidation of Fe<sub>3</sub>O<sub>4</sub>, but the total preparation process is cumbersome



Recently, to obtain  $\gamma$ -Fe<sub>2</sub>O<sub>3</sub> nanocrystals conveniently, many methods have been studied. For instance, Ziolo et al.<sup>4,8</sup> reported the matrix-mediated synthesis of  $\gamma$ -Fe<sub>2</sub>O<sub>3</sub> nanocrystals in aqueous solution using FeCl<sub>2</sub>·4H<sub>2</sub>O as raw material. Chhabra et al.<sup>7</sup> also prepared nanocrystalline  $\gamma$ -Fe<sub>2</sub>O<sub>3</sub> particles from a microemulsion-mediated reaction. Chen and Xu<sup>17</sup> successfully fabricated  $\gamma$ -Fe<sub>2</sub>O<sub>3</sub> nanocrystals employing the hydrothermal synthesis route. However, relatively high temperature or long reaction time was needed in these methods and the obtained products were often spherical particles. In this paper, we design a simple and novel room-temperature reduction–oxidation route for the preparation of  $\gamma$ -Fe<sub>2</sub>O<sub>3</sub> nanocrystals based on the characteristic of Fe(0) atom of being easily oxidized by air. The reactions

\* To whom correspondence should be addressed. E-mail: xwge@ustc.edu.cn.

(1) Mann, S.; Hannington, J. P. *J. Colloid Interface Sci.* **1988**, *122*, 326.

(2) Zhao, X. K.; Herve, P. J.; Fendler, J. H. *J. Phys. Chem.* **1989**, *93*, 908.

(3) Papaefthymiou, V.; Kostikas, A.; Simopoulos, A.; Niarchos, D.; Gangopadhyay, S.; Hadjipanayis, G. C.; Sorensen, C. M.; Klabunde, K. *J. Appl. Phys.* **1990**, *67*, 443.

(4) Ziolo, R. F.; Giannelis, E. P.; Weinstein, B. A.; Ohoro, M. P.; Ganguly, B. N.; Mehrotra, V.; Russell, M. W.; Huffman, D. R. *Science* **1992**, *257*, 219.

(5) Takahashi, N.; Kakuda, N.; Ueno, A.; Yamaguchi, K.; Fujii, T. *Jpn. J. Appl. Phys.* **1987**, *28*, 244.

(6) Jones, H. E.; Bissell, P. R.; Chantrell, R. W. *J. Magn. Magn. Mater.* **1990**, *83*, 455.

(7) Chhabra, V.; Ayyub, P.; Chattopadhyay, S.; Maitra, A. N. *Mater. Lett.* **1996**, *26*, 21.

(8) Kroll, E.; Winnik, F. M.; Ziolo, R. F. *Chem. Mater.* **1996**, *8*, 1594.

(9) Kang, Y. S.; Risbud, S.; Rabolt, J. F.; Stroeve, P. *Chem. Mater.* **1996**, *8*, 2206.

(10) Gunther, L. *Phys. World* **1990**, *3*, 28.

(11) Marignier, J. L.; Belloni, J.; Delcourt, M. O.; Chevalier, J. P. *Nature* **1985**, *317*, 344.

(12) (a) Michaelis, M.; Henglein, A. *J. Phys. Chem.* **1992**, *96*, 4719. (b) Henglein, A.; Ershov, B. G.; Malow, M. *J. Phys. Chem.* **1995**, *99*, 14129.

(13) Qian, Y.; Zhu, Y.; Zhang, M.; Chen, Z. *Micro- Nanometer Sci. Technol. (China)* **1995**, *1*, 27.

(14) Liu, H. R.; Ge, X. W.; Xu, X. L.; Zhang, Z. C.; Zhang, M. W. *Radiat. Phys. Chem.* **1999**, *55*, 357.

(15) Wang, S.; Xin, H. *Radiat. Phys. Chem.* **1999**, *56*, 567.

(16) Yin, Y.; Xu, X.; Ge, X.; Xia, Ch.; Zhang, Zh. *Chem. Commun.* **1998**, 1641.

(17) Chen, D.; Xu, R. *J. Solid State Chem.* **1998**, *137*, 185.

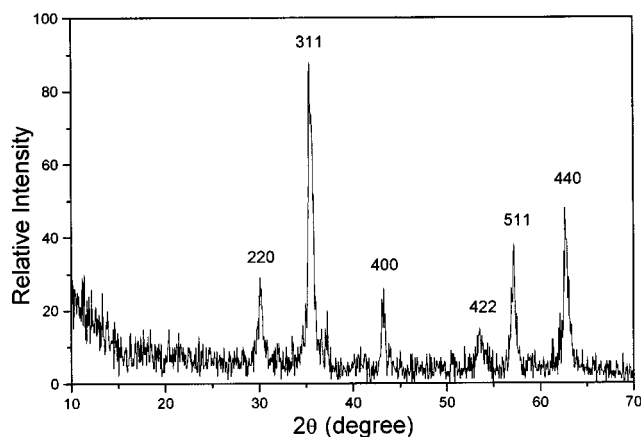


**Figure 1.** XRD pattern of the as-prepared  $\gamma$ -Fe<sub>2</sub>O<sub>3</sub> nanocrystals.

contain two steps: First, Fe(II) is reduced into Fe atoms by  $\gamma$ -ray irradiation in nitrogen atmosphere; then, Fe atoms are oxidized into  $\gamma$ -Fe<sub>2</sub>O<sub>3</sub> in air. All reactions occur at room temperature and under ambient pressure.

## 2. Experimental Section

In a typical experiment, appropriate amount of analytically pure FeSO<sub>4</sub>·7H<sub>2</sub>O was dissolved into distilled water. To scavenge some oxidative radicals such as  $\cdot$ OH produced during  $\gamma$ -ray irradiation and maintain the reductive atmosphere of the system, isopropyl alcohol, a scavenger of oxidative radicals, was also added into the system. After the solution had been bubbled with nitrogen for 40 min, NH<sub>3</sub>·H<sub>2</sub>O was introduced into the system to adjust pH value to above 11. Then the system was continuously bubbled with nitrogen for 20 min to remove oxygen. Finally the system was irradiated in the field of a  $2.22 \times 10^{15}$  Bq <sup>60</sup>Co  $\gamma$ -ray source with the absorption dose of 60 kGy at the dose rate of 50 Gy/min. After irradiation, the produced black precipitates were collected, placed in air for 24 h, washed with distilled water several times, and dried in air at room temperature.

The phase of the as-prepared product was identified by X-ray powder diffraction (XRD) patterns employing a scanning rate of 0.02°/s in  $2\theta$  range from 10 to 70°, using a Japan Rigaku D/max  $\gamma_A$  X-ray diffractometer equipped with graphite monochromatized Cu K $\alpha$  radiation ( $\lambda = 0.154178$  nm). The morphology and particle size of the product were determined by transmission electron microscopy (TEM), which was taken on a Hitachi model H-800 transmission electron microscope with an accelerating voltage of 200 kV. Mössbauer spectrum (MS) was recorded on the MS-500 spectrometer at room temperature in constant acceleration mode between -10 and 10 mm/s. Energy-dispersed X-ray analysis (EDXA) of the final product was taken on a JEOL-2010 transmission electron microscope using an accelerating voltage of 200 kV. The surface valences and the composition of the final product were analyzed according to X-ray photoelectron spectra (XPS) of the sample, which were recorded on an ESCA Lab MKII instrument with Mg K $\alpha$  radiation as the exciting source. A direct current B-H magnetometer made in Shanghai (VSM-9500) was used to evaluate the magnetic properties at room temperature.

## 3. Results and Discussions

The XRD pattern of the as-prepared product is given in Figure 1. According to the Scherrer's equation, the mean size of the product is calculated to be about 27 nm. No other compound peak appears in Figure 1. However, since the XRD patterns of  $\gamma$ -Fe<sub>2</sub>O<sub>3</sub> and Fe<sub>3</sub>O<sub>4</sub> are very similar, it is difficult to distinguish the two phases simply from XRD patterns. Even so, comparing

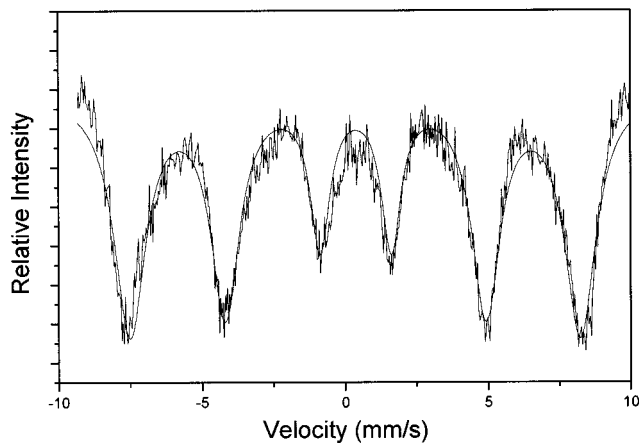


**Figure 2.** Mössbauer absorption spectrum of the final product measured at room temperature.

**Table 1. The  $d$  Values of the As-prepared Sample and JCPDS Card Nos. 39-1346 and 19-629**

	sample	no. 39-1346	no. 19-629	$hkl$
$d$ value	2.9497	2.953	2.967	220
	2.5149	2.5177	2.532	311
	2.0849	2.0886	2.0993	400
	1.7039	1.7045	1.7146	422
	1.6078	1.6073	1.6158	511
	1.4754	1.4758	1.4845	440

with the  $d$  values of the experiment and JCPDS card nos. 39-1346 and 19-629 (see Table 1), one can find that the result of the experiment is much closer to that of no. 39-1346. To ascertain the phase of the final product, the Mössbauer spectrum (MS) of the sample shown in Figure 1 was measured. Since the MS of  $\gamma$ -Fe<sub>2</sub>O<sub>3</sub>, which is a sextet peak,<sup>18</sup> obviously differs from that of Fe<sub>3</sub>O<sub>4</sub>, which is two sextet peaks,<sup>19</sup> the form of the final product can be discriminated. Figure 2 shows the experimental and calculated MS of the as-prepared product. The corresponding hyperfine parameters are  $\delta = 0.328$  mm/s,  $\langle QS \rangle = 1.032$  mm/s, which are typical of iron(III).<sup>18</sup> The broad lines of the magnetic sextets and the smooth inner slopes suggest the existence of a wide size distribution of the obtained iron oxide. At the same time, the form of the final product is further proved by EDXA. Figure 3 gives two patterns of EDXA obtained in two different areas. The element ratio of Fe:O is calculated to be 41.75:58.25 and 37.67:62.33, respectively, which are very close to the stoichiometry of Fe<sub>2</sub>O<sub>3</sub>. In Figure 3, the appearance of Cu peaks results from copper net used in the experiment.

In addition, the oxidation-reduction titration method<sup>20</sup> was also used to analyze the content of iron in the final product. First, an appropriate amount of final product was dissolved with heat in HCl aqueous solution with the volume ratio of 1:1 (HCl:H<sub>2</sub>O). Then, Fe<sup>3+</sup> ions were reduced to Fe<sup>2+</sup> ions, employing SnCl<sub>2</sub> as the reductant. Finally, Fe<sup>2+</sup> ions were titrated with 0.1002 mol/L K<sub>2</sub>Cr<sub>2</sub>O<sub>7</sub> standard solution in a mixed solution of 1mol/L H<sub>2</sub>SO<sub>4</sub> and H<sub>3</sub>PO<sub>4</sub>, using sodium diphenylamine sulfonate as the indicator. Here, H<sub>3</sub>PO<sub>4</sub> was used mainly for

(18) Pascal, C.; Pascal, J. L.; Favier, F.; Moubtassim, M. L. E. *Chem. Mater.* **1999**, *11*, 141.

(19) Panda, R. N.; Gajbhiye, N. S.; Balaji, G. *J. Alloys Compd.* **2001**, *326*, 50.

(20) *Analytic Chemistry*, Version 2; ed. mainly by Wuhan University; Higher Education Publication: China, 1982; p 382.

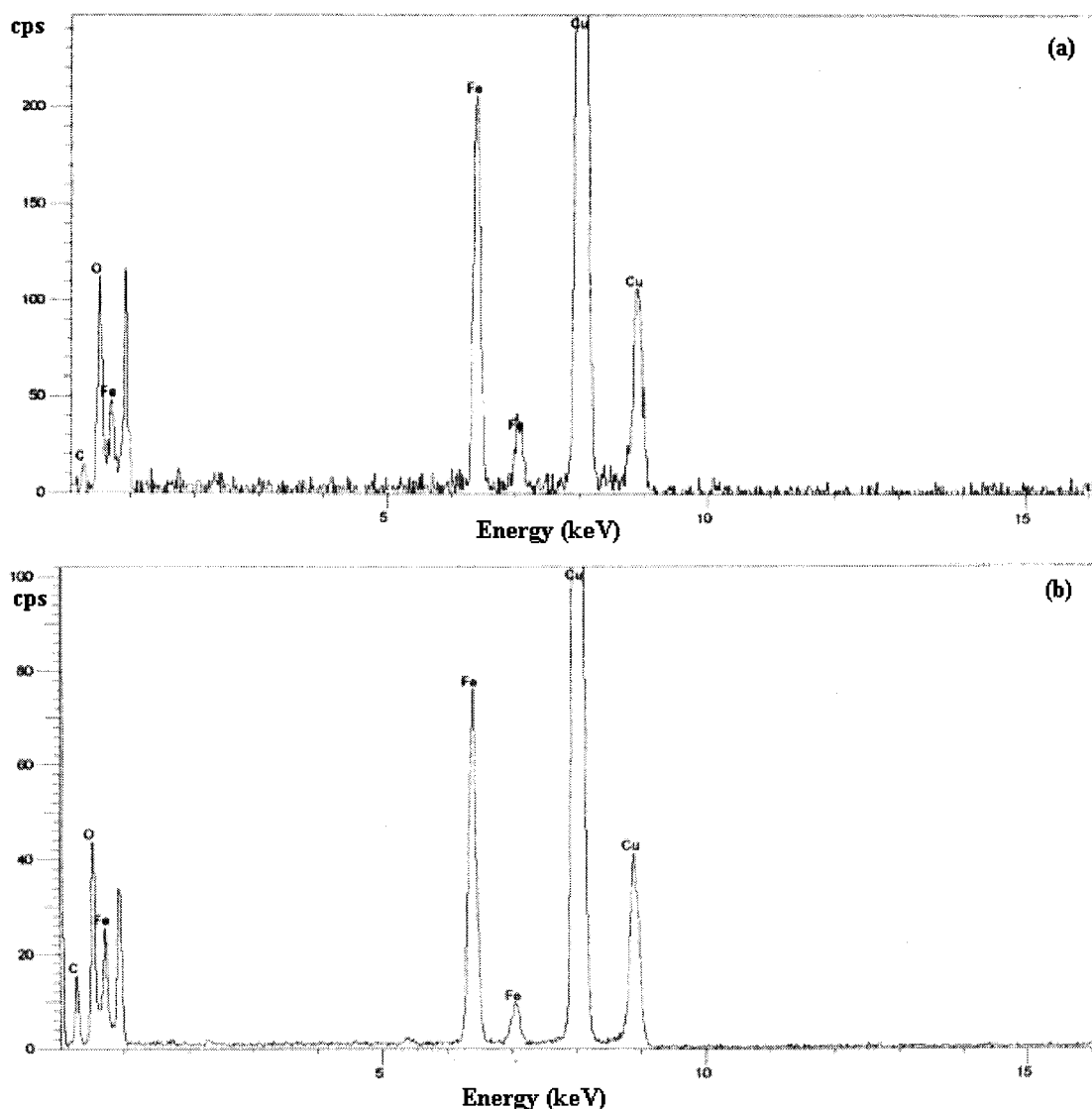


**Figure 3.** EDXA patterns of the final product obtained in two different areas: (a) 41.75:58.25 and (b) 37.67:62.33.

**Table 2. The Process and Results of Chemical Analysis**

expt no.	content of sample (g)	vol of 0.1002 mol/L $K_2Cr_2O_7$ consumed (mL)	mole ratio of Fe:O	avg mole ratio of Fe:O
1	1.0342	12.4	1:1.486	1:1.489
2	1.1008	13.1	1:1.497	
3	1.0097	12.1	1:1.484	

following reasons: since it can react with  $Fe^{3+}$  ions obtained during chemical titration to produce stable  $Fe(HPO_4)_2^-$  ions. Thus, the potential of  $Fe^{3+}/Fe^{2+}$  ( $E_{Fe^{3+}/Fe^{2+}}$ ) will be decreased and the error of experiments will also be reduced. Moreover, since  $Fe(HPO_4)_2^-$  ions have no color in aqueous solution, the change of the color of the indicator will not be disturbed and the sensitivity of the indicator will be enhanced. The above experiment was repeated three times, and the final results are listed in Table 2. As seen in Table 2, an average element ratio of Fe:O is about to be 1:1.489, which is very close to the stoichiometry of  $Fe_2O_3$ . This result also further confirms that the final product is the cubic  $\gamma$ - $Fe_2O_3$  phase.

TEM images of the final product are shown in Figure 4. As seen in Figure 4a,  $\gamma$ - $Fe_2O_3$  powders consist of many rodlike crystals with various dimensions. In Figure 4b, however, a kind of plate-shaped structure is found. We

consider that the morphology of the final product should be plate shaped, and this kind of rodlike structure was formed only by the overlap of the plate-shaped  $\gamma$ - $Fe_2O_3$  nanocrystals. In the meantime, it is difficult to measure the dimensions of the final product in the TEM images due to this kind of a plate-shaped structure.

Figure 5 shows magnetic characterization of the  $\gamma$ - $Fe_2O_3$  nanoparticles, which was measured at room temperature. The as-prepared  $\gamma$ - $Fe_2O_3$  nanocrystals have a specific saturation magnetization of 83 emu/g, and the coercivity of the product is as high as 320 Oe (25.5 kA/m).

Figure 6 is the XPS pattern of the product. The results of Fe 2p<sub>3/2</sub>, Fe 2p<sub>1/2</sub>, and O 1s electron binding energies are shown in Figure 6 and Table 3, which are very similar to the values recorded in the literature.<sup>21</sup> Through calculation of peak area, the atom ratio of Fe and O is about 2:3. As seen in Table 3, the valences of Fe and O are +3 and -2 in proper order.

A possible formation process of the plate-shaped  $\gamma$ - $Fe_2O_3$  nanocrystals was suggested according to the

(21) Fujii, T.; de Groot, F. M. F.; Sawatzky, G. A.; Voogt, F. C.; Hibma, T.; Okada, K. *Phys. Rev. B* **1999**, *59*, 3195.

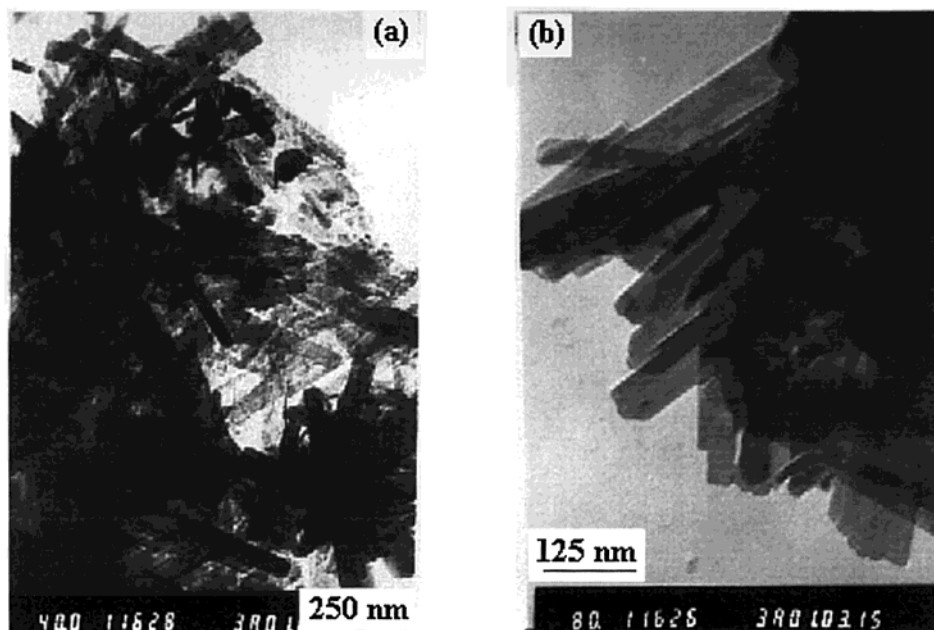


Figure 4. TEM images of  $\gamma$ -Fe<sub>2</sub>O<sub>3</sub> nanocrystals: (a) rodlike structure and (b) plate-shaped structure.

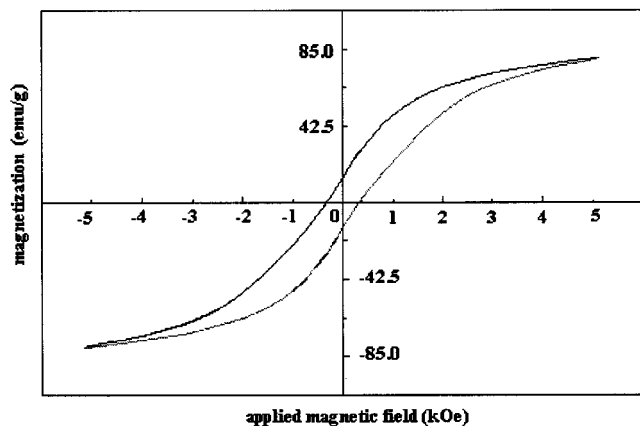


Figure 5. Hysteresis measurements of  $\gamma$ -Fe<sub>2</sub>O<sub>3</sub> nanocrystals at room temperature.

designed route. First, the Fe<sup>2+</sup> ions reacted with NH<sub>3</sub>·H<sub>2</sub>O to produce Fe(OH)<sub>2</sub> in nitrogen atmosphere. Then, the system was irradiated by  $\gamma$ -rays. Many active products were generated during the radiolysis of water



Among these active products, the hydrated electron and the hydrogen atom were strong reductive particles. They could reduce Fe(OH)<sub>2</sub> into iron atoms. Meanwhile, some oxidative particles such as hydroxyl radicals could prevent the iron atoms from producing and must be scavenged, so isopropyl alcohol was introduced into the system. Although the hydrogen atoms could be also scavenged by isopropyl alcohol, the reducing reaction was not affected since Fe(OH)<sub>2</sub> was reduced mainly by the hydrated electron

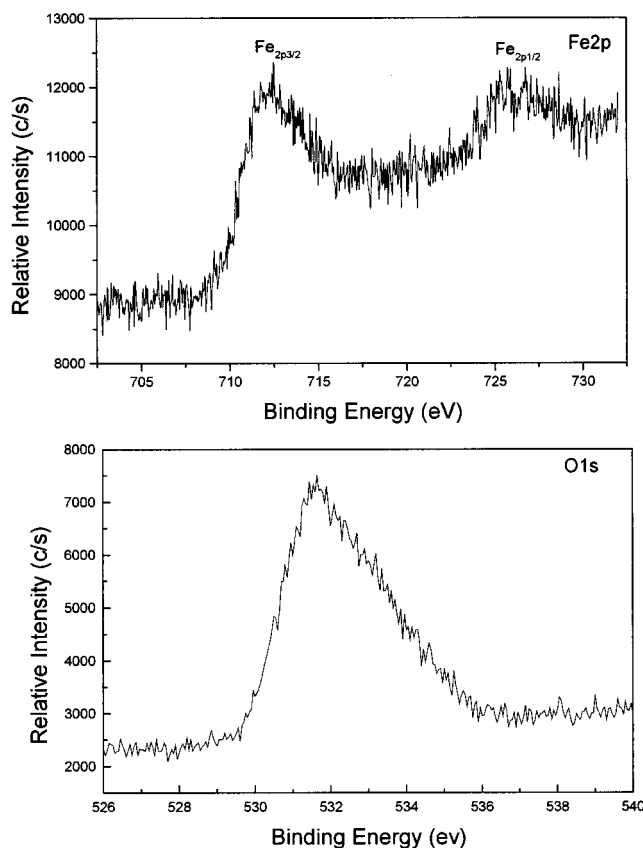
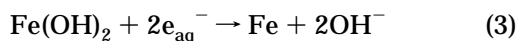
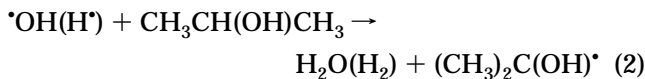


Figure 6. XPS patterns of the product.

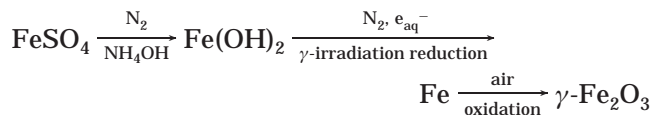
Table 3. Binding Energies and Valences of the Final Product

electron level	binding energy (eV)	valence
Fe 2p <sub>3/2</sub>	711.7	+3
Fe 2p <sub>1/2</sub>	725.5	
O 1s	531.7	-2

Since the new radicals produced in eq 2 were also reductive, the reducing atmosphere of the system was maintained and the yield of iron atoms was further



improved. Although the yielded iron atoms were very active, they could exist in the basic and reducing conditions. However, during the reduction of  $\text{Fe}(\text{OH})_2$ , since a layer-shaped structure existed between  $\text{Fe}^{2+}$  and  $\text{OH}^-$  ions in  $\text{Fe}(\text{OH})_2$ ,<sup>22</sup>  $\text{Fe}^{2+}$  ions could be attacked only along certain direction by the hydrated electrons. Thus, it was possible that the produced iron particles had a certain shape. When these iron particles were treated in air, they were quickly oxidized by oxygen in air. Thus, the plate-shaped  $\gamma\text{-Fe}_2\text{O}_3$  nanocrystals were obtained. This process can be written in a simplified way



#### 4. Conclusion

The plate-shaped  $\gamma\text{-Fe}_2\text{O}_3$  nanocrystals have been successfully prepared in aqueous solution through a

simple reduction–oxidation route at room temperature and under constant pressure. No extra reducing reagent was introduced into the system owing to the usage of the  $\gamma$ -ray irradiation technique, and the obtained product could be easily collected and treated. No  $\alpha\text{-Fe}_2\text{O}_3$  phase was shown in the XRD pattern of the sample. Although the XRD pattern of  $\text{Fe}_3\text{O}_4$  is very close to that of  $\gamma\text{-Fe}_2\text{O}_3$ , there are obvious differences in their Mössbauer spectra. Furthermore, the final product was also proved to be a highly pure  $\gamma\text{-Fe}_2\text{O}_3$  form by EDXA and chemical analysis. The researches indicated that the experiment would not succeed till three conditions were realized—nitrogen protection, basic condition, and reductive atmosphere.

**Acknowledgment.** We are grateful for the support of the Young Fund of University of Science and Technology of China and the Fund of Doctoral position (WJ1201).

(22) Goto, H.; Alashi, G. *U.S. Patent* 3,047,428, 1962.